JPCBFK

VOLUME 110
AUGUST 17, 2006
NUMBER 32
http://pubs.acs.org/JPCB

THE JOURNAL OF PHYSICAL CHEMISTRY B

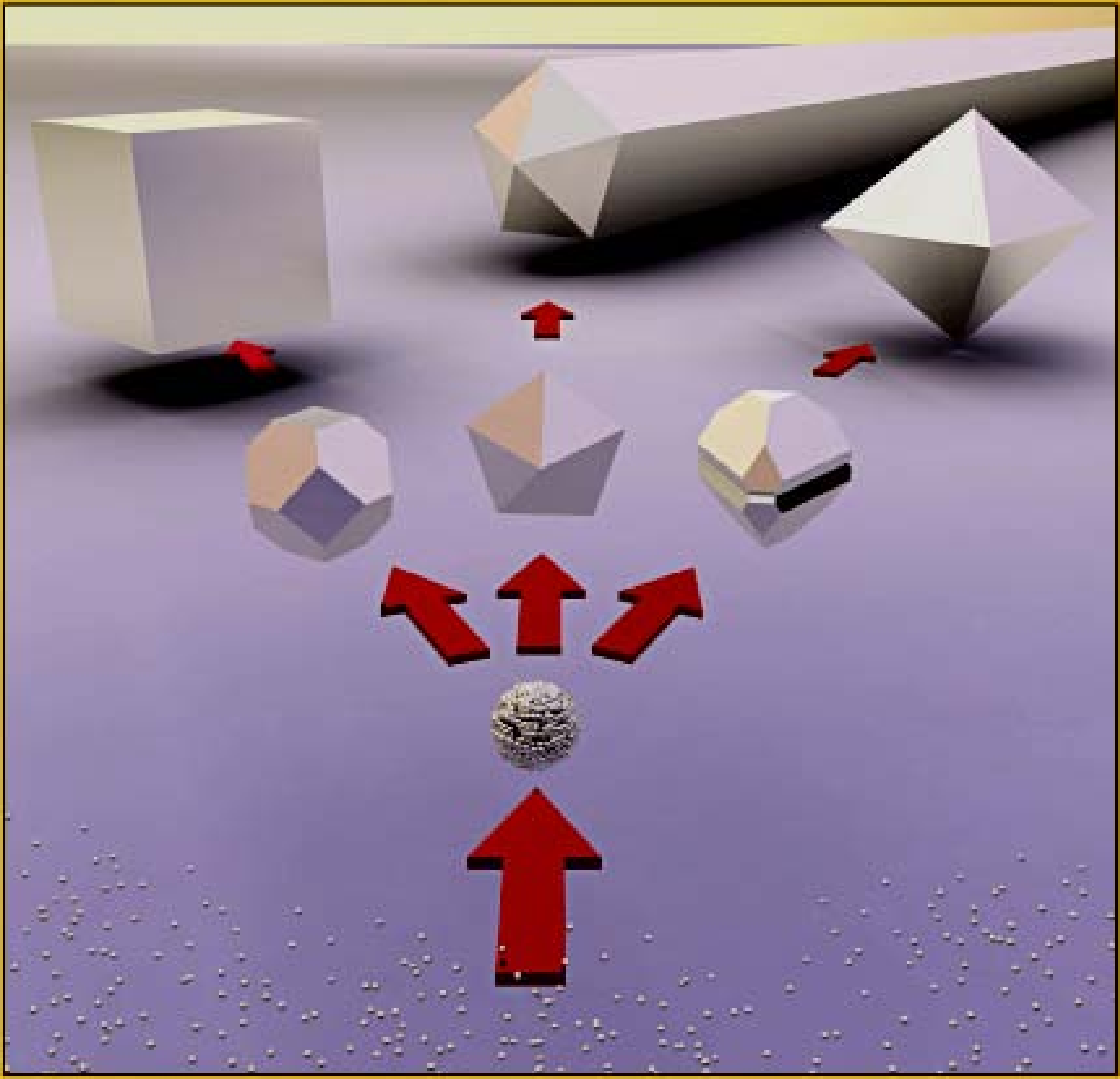

Directed Assembly of Silver Atoms to Produce Silver Nanostructures with Unique Plasmonic Properties (see page 15666)

CONDENSED MATTER, MATERIALS, SURFACES, INTERFACES, & BIOPHYSICAL CHEMISTRY

PUBLISHED WEEKLY BY THE AMERICAN CHEMICAL SOCIETY

FEATURE ARTICLE

Maneuvering the Surface Plasmon Resonance of Silver Nanostructures through Shape-Controlled Synthesis

Benjamin J. Wiley,[†] Sang Hyuk Im,[‡] Zhi-Yuan Li,[§] Joeseph McLellan,[‡] Andrew Siekkinen,[‡] and Younan Xia*,[‡]

Departments of Chemical Engineering and Chemistry, University of Washington, Seattle, Washington 98195, and Institute of Physics, Chinese Academy of Sciences, Beijing 100080, P. R. China

Received: February 9, 2006; In Final Form: April 21, 2006

Silver nanostructures are containers for surface plasmons − the collective oscillation of conduction electrons in phase with incident light. By controlling the shape of the container, one can control the ways in which electrons oscillate, and in turn how the nanostructure scatters light, absorbs light, and enhances local electric fields. With a series of discrete dipole approximation (DDA) calculations, each of a distinctive morphology, we illustrate how shape control can tune the optical properties of silver nanostructures. Calculated predictions are validated by experimental measurements performed on nanocubes with controllable corner truncation, right bipyramids, and pentagonal nanowires. Control of nanostructure shape allows optimization of plasmon resonance for molecular detection and spectroscopy.

Introduction

How does light interact with matter? This was the question Michael Faraday tried to answer through his examination of metal colloids. He was the first to show that metal particles many times smaller than the wavelength of light nonetheless scatter and absorb light strongly, such that even dilute solutions exhibit bright colors.[1] As an inventor of the dynamo, Faraday would have been intrigued to know that the collective oscillation of conduction electrons within metal particles enables scattering and absorption of light at a particular frequency, giving them color in the case of silver and gold. This collective oscillation of conduction electrons is now known as surface plasmon resonance (SPR). S*urface* denotes the polarization of surface charges resulting from collective electron oscillations, and *plasmon* is in analogy to the collective electron oscillations within gaseous plasma.[2] When excited by light, the induced charges characteristic to surface plasmons can propagate as an electromagnetic wave along the surface of bulk gold or silver. The oscillating charges can also be confined and enhanced on the surface of a nanoparticle, in which case it is called localized surface plasmon resonance (LSPR).

The fundamental relationship between surface plasmons and light continues to be explored, but the applications of SPR, both those already developed and those on the horizon, drive the great interest in this field. SPR biosensing, for which commercial products are sold, relies on the principle that the angle at which light reflects from a gold film responds to the polarizability of the surrounding medium, and thus to the presence of biomolecules on the gold surface.[3] This technique allows not only label-free detection of biomolecules, but also quantification of their interaction kinetics, and thus is widely used in both clinical and research settings. In an effort to reduce the detection limit of SPR biosensing to zeptomoles (10^{-21} moles per liter), Van Duyne and co-workers have focused on detecting adsorbate-induced changes in the light scattered from a single silver nanoparticle.[4] LSPR also creates intense electric fields within a few nanometers of a nanoparticle surface. This near-field enhances the Raman scattering of adsorbed molecules, providing a “fingerprint” spectrum containing rich chemical information.[5,6] Furthermore, localized surface plasmons can be guided and focused below the diffraction limit of light with arrays of silver nanoparticles or nanoscale holes in silver films.[7−9] Silver nanostructures can also be combined with photosensitive polymers to image the near fields surrounding a silver nanostructure and perform nanoscale lithography.[10,11]

In this feature article we focus on the most powerful way to tune the LSPR characteristics of a metal nanostructure − control of shape. We will specifically address only nanostructures of silver as they scatter light and enhance near-fields an order of magnitude more strongly than do those of gold.[12,13] It has been known for nearly 100 years that the shape of a nanoparticle will affect its interaction with light, but only within the past decade has it become possible to control the shape of silver nanoparticles synthesized in solution. To demonstrate the specific ways in which shape affects the absorption and scattering of light, we have performed discrete dipole approximation calculations for ten different shapes, most of which have not been reproduced elsewhere. We then discuss how we have synthesized silver nanostructures in solution, including examples of nanocubes with controllable corner truncation, right bipyramids, and pentagonal nanowires. The UV−vis spectra taken from synthesized nanostructures confirm several trends

---

* Corresponding author. E-mail: xia@chem.washington.edu

[†] Department of Chemical Engineering, University of Washington.

[‡] Department of Chemistry, University of Washington.

[§] Chinese Academy of Sciences.

10.1021/jp0608628 CCC: $33.50 © 2006 American Chemical Society
Published on Web 06/30/2006

Benjamin J. Wiley received a B.S. in chemical engineering from the University of Minnesota in 2003, before joining the Xia group at the University of Washington. His research focuses on the synthesis and characterization of metallic nanostructures, as well as their biomedical applications. He is a recipient of an NSF IGERT fellowship from the Center for Nanotechnology at UW.

Sang Hyuk Im received his B.S., M.S., and Ph.D. degrees in chemical and biomolecular engineering from the Korea Advanced Institute of Science and Technology (KAIST) in 1998, 2000, 2003, respectively. He then worked as a postdoctoral fellow in the Xia group at the University of Washington until 2005. Now he is working as a senior research scientist in the LG Chemicals Research Park. His research interests include self-assembly of colloidal nanoparticles, structure and morphology control of organic and inorganic materials, and development of advanced functional coating materials such as hard, antistatic, antifouling, and antireflection coatings for flat-panel displays.

Zhi-Yuan Li received a B.S. in optoelectronics from the University of Science and Technology (USTC) in 1994 and a Ph.D. in optics from the Institute of Physics, Chinese Academy of Sciences in 1999. After several years of postdoctoral experiences in the U.S., he joined the Institute of Physics, Chinese Academy of Sciences in 2004 and is now a professor and deputy director of the Optical Physics Laboratory. His current research focuses on the optical physics of photonic crystals, negative refraction materials, and metallic nanostructures. He is the author or coauthor of more than 100 peer-reviewed journal articles. Li can be reached at lizy@aphy.iphy.ac.cn.

Joseph McLellan received his B.S. and M.S. in chemistry from Western Washington University in 2001 and 2003, respectively. His graduate work at Western focused on the use of liquid crystals as templates for growth of organic semiconductors. Since 2003 he has been a graduate student in the Xia group at the University of Washington. His scientific interests include novel surface patterning and fabrication techniques, nanoparticle synthesis, self-assembly, and surface-enhanced Raman spectroscopy.

Andrew R. Siekkinen received a B.A. in chemistry from Hiram College in 2004. His research has included developing ELISA methods for pesticide detection as a NSF-REU student at Virginia Commonwealth University in 2003. He has also worked with heat exchanger, fuel reformer, and catalytic combustor catalysts at Catacel Corporation from 2003 until beginning his graduate studies at the University of Washington in 2004. His current research in the Xia group focuses on developing syntheses and applications of inorganic nanoparticles.

Younan Xia was born in Jiangsu, China, in 1965. He received a B.S. degree in chemical physics from the University of Science and Technology of China (USTC) in 1987, and then worked as a graduate student on nonlinear optical materials for four years at the Fujian Institute of Research on the Structure of Matter, Chinese Academy of Sciences. He came to the United States in 1991, received an M.S. degree in inorganic chemistry from the University of Pennsylvania (with Professor Alan G. MacDiarmid) in 1993, and a Ph.D. degree in physical chemistry from Harvard University (with Professor George M. Whitesides) in 1996. He stayed at Harvard and worked as a postdoctoral fellow with Professors George M. Whitesides and Mara Prentiss. He moved to Seattle in 1997 and started as an Assistant Professor of Chemistry at the University of Washington. He was promoted to the rank of tenured Associate Professor in 2001 and to the rank of Professor in 2003. His research interests include nanostructrued materials, self-assembly, photonic crystals, colloidal science, microfabrication, surface modification, electrospinning, conducting polymers, microfluidic and microanalytical systems, and novel devices for photonics, optoelectronics, and displays.

predicted by the calculations and should give the reader an intuitive understanding of the interaction between shape, plasmon resonance, and light. We end this article with preliminary applications of these nanostructures that illustrate how they could be utilized in molecular sensing.

Theory and Calculation

Gustav Mie was the first to rigorously explain the colors exhibited by metal colloids with Maxwell's equations.[14] However, because exact solutions to Maxwell's equations are known only for spheres, shells, spheroids, and infinite cylinders, an approximation is required to solve the equations for other geometries. The approximation of choice is called the discrete dipole approximation (DDA).[15] In a DDA calculation, the nanoparticle is discretized into a cubic array of N polarizable points, with each point representing the polarizability of a discrete volume of material. The presence of an electromagnetic field (light) gives these points a dipole moment. In the steady-state limit, each dipole is polarized by an electric field that includes contributions from the incident light and every other dipole in the array. The polarization at each point ($\mathbf{P}_j$) must thus be calculated through an iterative procedure, which can be accelerated with FFT methods (thus the periodicity of the array). $\mathbf{P}_j$ can then be plugged into an equation to determine the scattering and absorption cross-sections of the particle, which in turn are divided by the cross-sectional area to give the dimensionless optical coefficients. As the coefficients can be solved exactly for this N-point array, the only approximation is in the number of points. A greater N increases the accuracy of the calculation at the expense of computation time. To ensure accuracy, the simulations presented here use dipoles no more than 2 nm in length and separation.

Figure 1A shows the UV−vis extinction, absorption, and scattering spectra (note: extinction = absorption + scattering) for a 40-nm silver sphere in water calculated via Mie theory. This calculation shows that silver nanospheres of this size

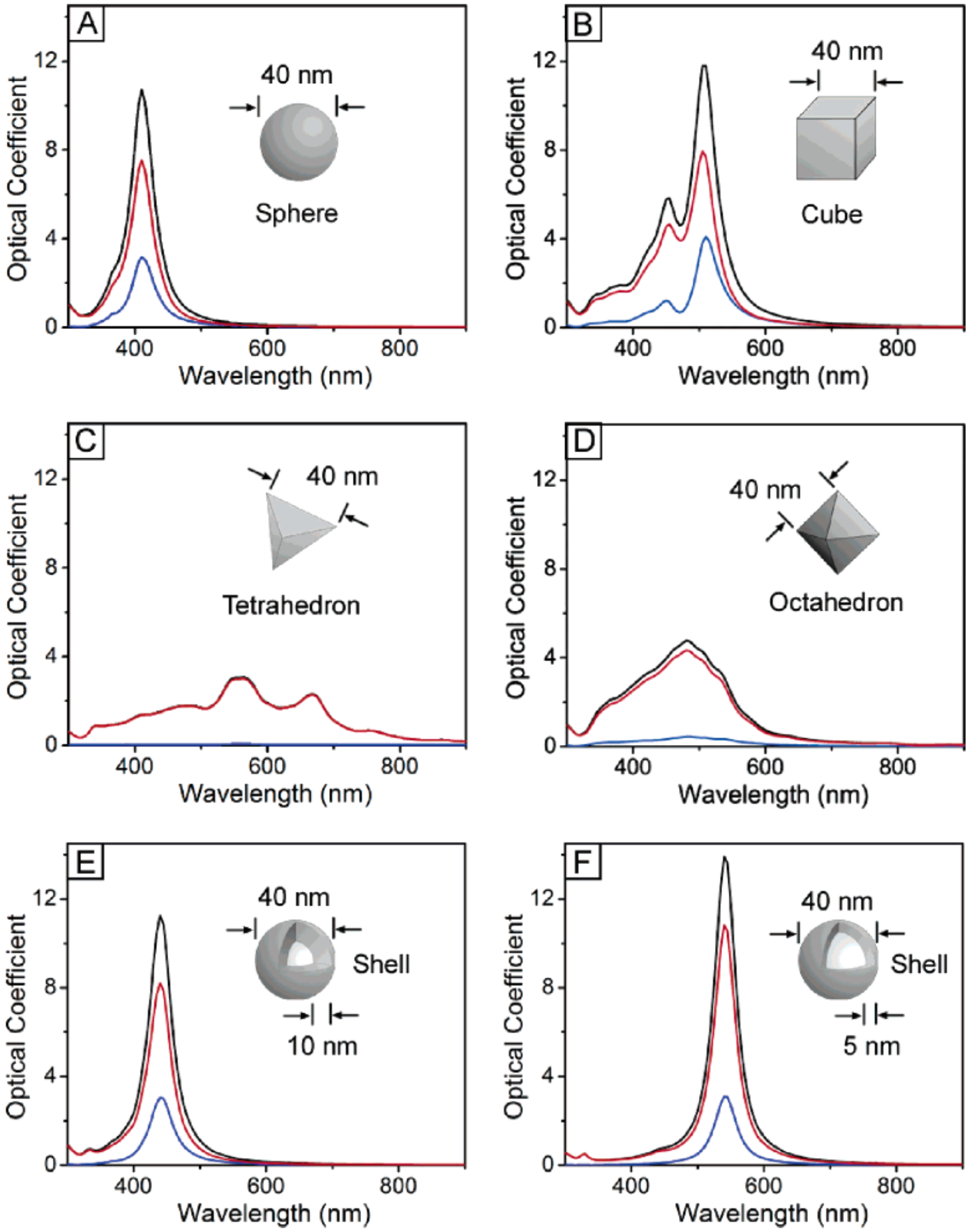

Figure 1. Calculated UV−vis extinction (black), absorption (red), and scattering (blue) spectra of silver nanostructures, illustrating the effect of a nanostructure's shape on its spectral characteristics. An isotropic sphere (A) exhibit spectra with a single resonance peak. Anisotropic cubes (B), tetrahedra (C), and octahedra (D) exhibit spectra with multiple, red-shifted resonance peaks. The resonance frequency of a sphere red-shifts if it is made hollow (E), with further red-shift for thinner shell walls (F).

primarily absorb blue light, letting the red and green wavelengths combine to give silver sols their characteristic yellow color. The spectrum shows the presence of two resonance peaks: the main dipole resonance peak at 410 nm, and a smaller quadrupole resonance at 370 nm present as a shoulder. The dipole resonance arises from one side of the sphere surface being positively charged while the opposite side is negatively charged, giving the particle itself a dipole moment that reverses sign at the same frequency as the incident light.[2] Energy losses make the incident light nonuniform across the sphere and induce a weak quadrupole resonance, characterized by two parallel dipoles of opposite sign. Surface polarization (i.e., charge separation) is the most important factor in determining the frequency and intensity of plasmon resonance for a given metal because it provides the main restoring force for electron oscillation.[2] Indeed, any variation in particle size, shape, or dielectric environment will change the surface polarization and thus the resonance peak.

The DDA calculated spectra of a 40-nm cube (Figure 1B) exhibits more peaks than the sphere because the cube has several distinct symmetries for dipole resonance compared with only one for the sphere.[16] The most intense peak is red-shifted compared with that of the sphere, a phenomenon often observed for nanostructures with sharp corners.[17] Calculations of the near-fields around nanostructures show that surface charges accumulate at sharp corners.[18] This segregation of charges into corners increases charge separation, and thereby reduces the restoring force for electron oscillation.[19] The weaker restoring force in turn manifests itself in a red-shift of the resonance peak. Similar trends are observed for the tetrahedron (Figure 1C) and octahedron (Figure 1D), although they have reduced scattering

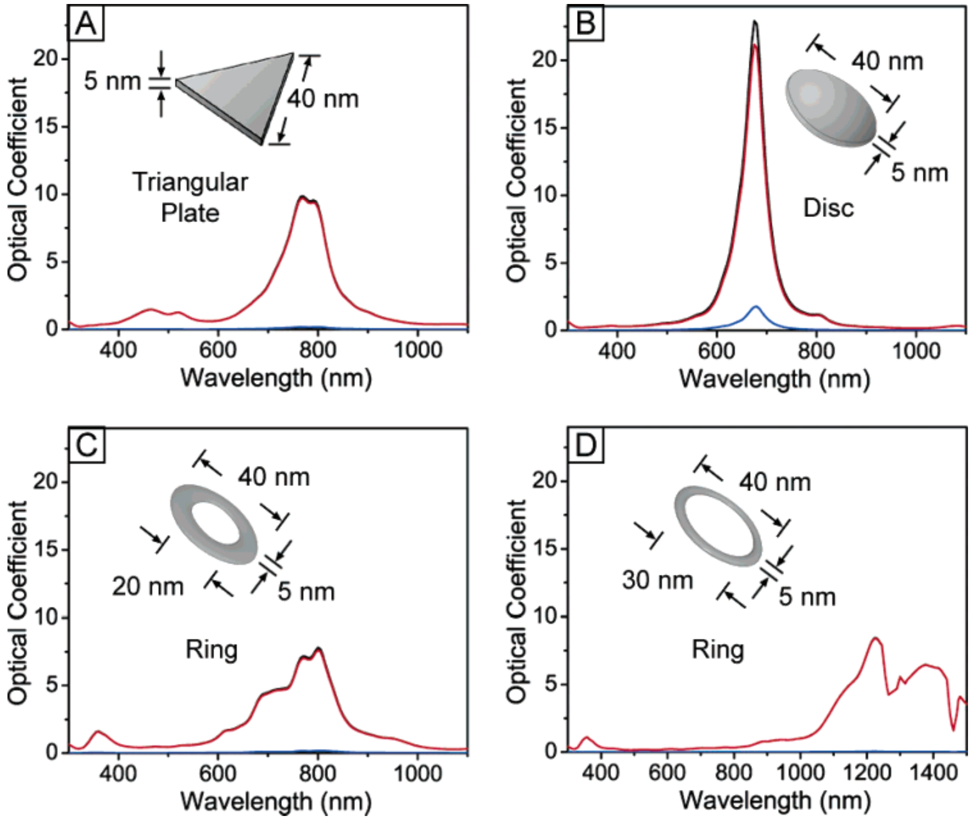

Figure 2. UV−vis−NIR extinction (black), absorption (red), and scattering (blue) spectra of silver nanostructures obtained using the DDA calculation. Spectra of a triangular plate (A) and circular disc (B) illustrate how resonance peaks red-shift for particles with 2D anisotropy. (C, D) Comparison of silver nanorings of two different thicknesses show that resonance peaks red-shift for thinner rings. Note that absorption dominates the spectra of these 2-D nanostructures.

cross-sections because of their different symmetries and smaller volumes. The tetrahedron has the most red-shifted resonance peaks of these three platonic solids because it has the sharpest corners. Although we do not display the origins of each peak here, they can be determined by plotting the induced polarization of dipoles at the resonance peak frequency via a DDA calculation.[20]

The calculated resonance peak of hollow spheres, or shells, is also red-shifted relative to that of a sphere (Figure 1E). In this case the incident electric field induces surface charges both inside and outside the shell.[21] The particle must have a dipole moment to compensate for the incident field, so charges on the inner surface are of the same sign as those on the outer surface for a given pole.[22] The increased charge separation reduces the frequency of oscillation. For thinner shells (Figure 1F), stronger coupling between charges inside and outside of the shell causes greater charge separation and further red-shift (Figure 1F). Calculations have shown that greater charge separation within shells gives them near-field enhancements four times those of spheres.[23]

Figure 2 presents the DDA calculations of several nanostructures with 2D anisotropy. These 2D nanostructures allow increased charge separation if polarized along their long axis, and thus they display peaks that are red-shifted from more isotropic nanostructures. Figure 2A shows the calculated spectra for a triangular nanoplate. In previous publications, the main dipole peak was shown to blue-shift if the corners of the nanoplates were snipped, clearly demonstrating that sharp corners result in a red-shifted resonance frequency.[20] The dipole resonance peak of the circular disc in Figure 2B is blue-shifted compared with the triangular plate because it lacks sharp corners, but the disc absorbs and scatters light more strongly because its circular symmetry gives it a larger effective dipole moment.[19] Thus, sharp corners always result in greater charge separation and a red-shifted resonance peak, but the intensity of the dipole resonance peak depends on the symmetry of the nanostructure. The effect of symmetry on peak intensity can also be observed by comparing the cube and tetrahedron. Charge separation into the corners of a cube will create a dipole because the corners are on opposite sides of a line of symmetry. The corners of a tetrahedron lay opposite a face instead of another corner, so no strong dipole is formed.

If the disc is transformed into a ring (Figure 2C), its resonance peak red-shifts for the same reasons as for the spherical shell, and the red shift increases with decreasing ring width (Figure 2D). The greater charge separation in the spherical shell relative to the sphere gives it a more intense resonance peak, but the resonance peak of rings is less intense than that of the disc, suggesting a smaller dipole moment. This has been previously observed in work that compared the spectra of gold discs and rings and may be related to the fact that the ring presents a smaller cross-sectional area to incident light.[24]

In summary, these DDA calculations clearly illustrate several ways in which the shape of a nanostructure affects the frequency and intensity with which the nanostructure scatters and absorbs light. First, the number of resonance frequencies exhibited by a nanostructure increases with the number of ways in which it can be polarized (i.e., when the structure has a lower symmetry). Second, resonance frequencies red-shift for nanostructures with increased corner sharpness, increased anisotropy, and decreased wall thickness (for hollow nanostructures). Third, the intensity of the resonance peak increases with an increase in the effective dipole moment of the particle, which is larger if charges separate with mirror symmetry. These rules can serve as a general

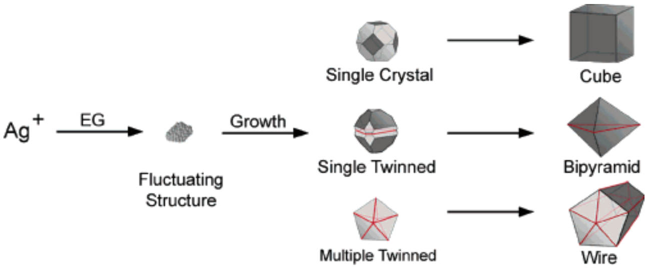

Figure 3. Illustration of the reaction paths leading to well-defined silver nanostructures. Ethylene glycol reduces silver ions to atoms, which form clusters of fluctuating structure. Fluctuation decreases as the cluster grows, until it evolves into a single-crystal, single twinned, or multiple twinned seed. Twins are delineated in the figure with red lines. Further growth of seeds can selectively enlarge (100) facets (dark gray) at the expense of (111) facets (light gray), resulting in formation of cubes, bipyramids, or wires.

guideline for design of metal nanostructures with properties specifically tuned for a desired application.

Synthesis and Characterization

Although lithographic methods have the ability to precisely define where a nanostructure is on a substrate, they do not come close to providing the same production capacity or level of control over nanostructure shape, size, and crystallinity as solution-phase synthesis. Triangular nanoplates, circular nanodisks, and nanowires of silver have all been synthesized with a combination of surfactants, reductants, and silver precursors in water.[25−27] Our own research has focused on the polyol synthesis, in which ethylene glycol (EG) serves as both solvent and reducing agent, as a general route to the production of silver nanocubes with controllable corner truncation, right bipyramids, and pentagonal nanowires.[28−30] This method has the attractive benefit that the reduction rate can be controlled by varying temperature.

In a typical synthesis, we heat EG in an oil bath set to 160 °C for 1 h before simultaneously injecting separate EG solutions of silver nitrate and poly (vinyl pyrrolidone) (PVP), with a molar ratio of PVP:Ag = 1.5. Note that the molar ratio is calculated in terms of the repeating unit of PVP. The PVP is added to the reaction to serve primarily as a stabilizer against aggregation, but it can also serve as a reductant and even plays a role in controlling the shape. The reduction does not occur without PVP, and well-defined silver nanostructures have not been produced by this system with other polymers.[31] Our experiments suggest that PVP interacts more strongly with silver atoms on {100} facets than with those on {111} facets, leading to nanostructures primarily bounded by this facet.[32] The final critical ingredient is the addition of Cl^-, Br^-, or Fe^{3+} to the PVP solution to produce nanocubes, right bipyramids, or nanowires of silver, respectively.

Within a minute after injection, silver ions are reduced to silver atoms, which in turn come together to form nuclei. At a small size, there is enough thermal energy for the structure of the nuclei to fluctuate, allowing defects to form or be removed depending on their energetic favorability.[33] Formation of twin defects, where a single atomic layer forms a mirror plane, is thermodynamically favored at small sizes because they enable a greater surface coverage of the lowest energy, {111} facet.[34] After nuclei grow past a certain size, changes in defect structure become too costly, and such seeds are stuck in a single crystal, single twin, or multiple twin morphology. These seeds can grow to become a cube, bipyramid, and wire, respectively. Figure 3 provides an illustrative summary of this growth process. The

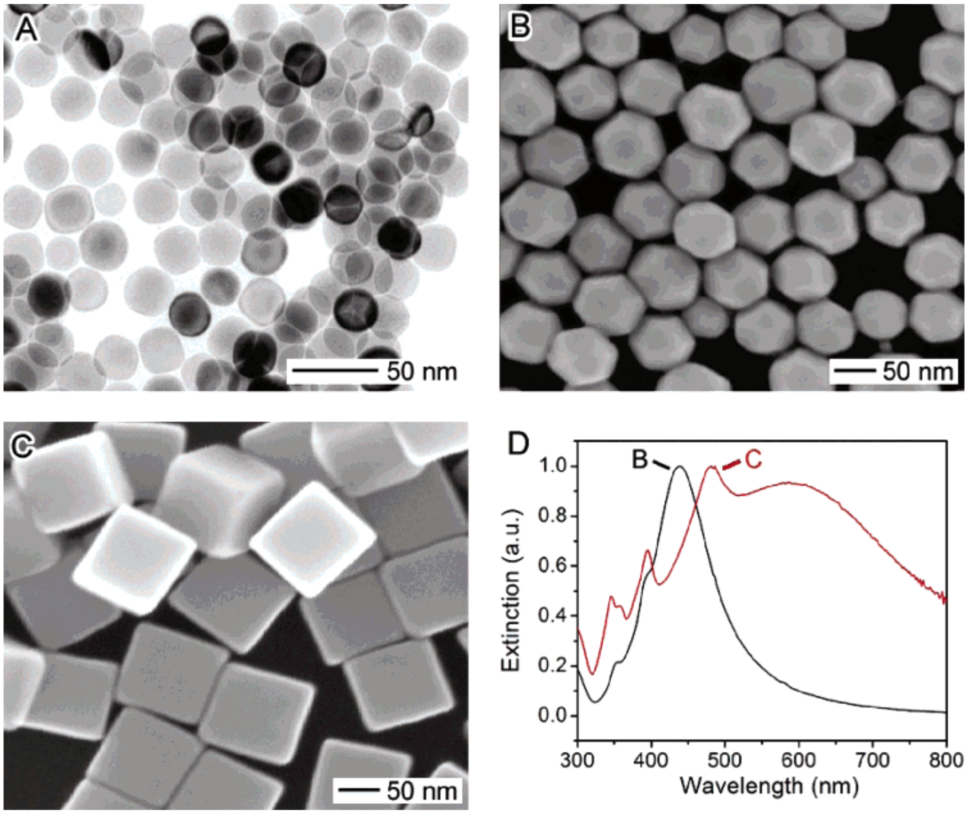

Figure 4. (A) TEM of single-crystal seeds that formed when NaCl was added to the synthesis. Chloride induced oxidative etching of twinned seeds. (B) SEM image of truncated nanocubes produced after 46 h in a reaction to which NaCl was added. (C) SEM of sharp nanocubes produced after 26 h in a reaction to which HCl was added. (D) The normalized UV−vis extinction spectrum of sharp cubes (C) is red-shifted and has several peaks, while the spectrum of the truncated cubes (B) more closely resembles the spectrum of a sphere. These results are reported in refs 35 and 38.

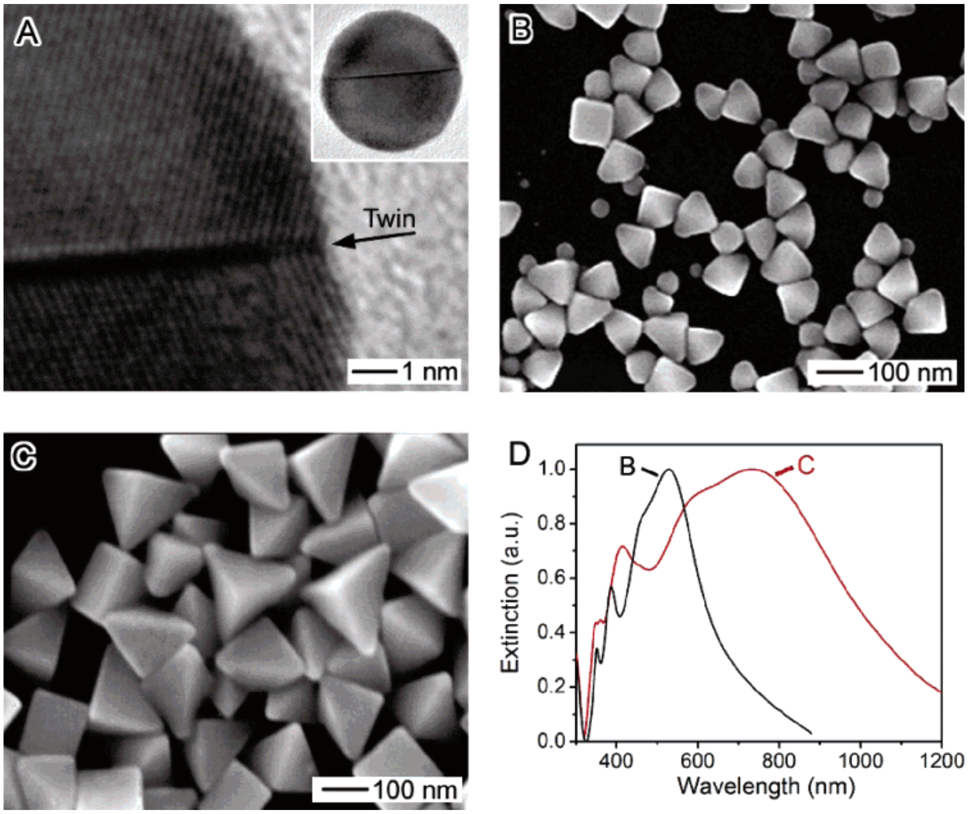

Figure 5. (A) HRTEM of a single twinned seed formed when NaBr was added in place of NaCl. Lattice fringes reflect across the (111) twin plane, denoted by an arrow. Single twin seeds grow to form right bipyramids (B) 75 nm (C) and 150 nm in edge length. (D) The normalized UV−vis spectrum of 75-nm bipyramids displays several distinct peaks, with the most intense peak being nearly 100 nm red-shifted from that of truncated cubes. The resonance peak shifted into the near-infrared region as the bipyramids grew to 150 nm. This work is expanded upon in ref 40.

key to obtaining only one of these shapes to the exclusion of others is to control the crystal structures of the seeds.

Figure 4A shows a TEM image of the ∼20 nm single-crystal nanoparticles produced after 24 h in a polyol synthesis to which chloride was added at a molar ratio of $Ag:Cl^- = 427$.[35] In the first few minutes of this reaction, the yellow color of the solution indicated the presence of silver nanoparticles, and a mixture of twinned and single-crystal nanoparticles could be found in TEM images of reaction samples. However, after a few hours the solution became clear and few such particles could be found, demonstrating that the addition of Cl^- had caused these silver nanoparticles to be etched. When the yellow color returned at $t = 24$ h, every nanoparticle was a single crystal. Because studies of silver catalysts have shown that higher defect density leads to greater activity for oxidation reactions, we propose it is the higher density of defects on the surface of twinned particles that led to their greater activity for oxidative etching.[36] If the reaction was performed under argon rather than air, the twinned particles formed in the early stage of the reaction grew quickly to form multiply twinned nanowires. If Cl^- was not added, micrometer-sized, multiply twinned spheroidal particles formed within 1 h. Thus both Cl^- and O_2 are required for formation of high yields of single-crystal seeds. Most recently, this oxidative etching mechanism was also validated for other noble metals including palladium, platinum, and rhodium.[37]

The single-crystal seeds can be grown into truncated (Figure 4B) or sharp (Figure 4C) cubes depending on the kinetics of the reduction. The truncated cubes took over 46 h to form, enough time for surface reconstruction to reduce surface area and increase the surface coverage of the lowest energy {111} facets on the corners, resulting in a more thermodynamically favored shape. If HCl rather that NaCl was added, sharp nanocubes formed after 26 h.[38] The faster growth that took place in this reaction resulted in a kinetically favored product, the sharp nanocube, bounded almost entirely by {100} facets. Addition of H^+ facilitated etching and made the reaction more robust, allowing it to be performed in a disposable vial. The vial was capped to reduce the level of oxygen in the later stages of the reaction, which reduced etching and allowed single crystal seeds to grow quickly into sharp nanocubes.

The normalized extinction spectra of truncated and sharp nanocubes suspended in water are compared in Figure 4D. The main dipole resonance peak for the 75 nm truncated nanocube is located at 440 nm, approximately the same location as for spheres of similar size.[39] At least two small shoulders in the spectra suggest the slight anisotropy of the truncated nanocube enables several distinct dipole resonances. These dipole resonances become more pronounced in the spectra for the 90-nm cubes with sharp corners, and the most intense peaks are red-shifted to as far as 600 nm. In comparison, the main peak exhibited by ∼90-nm spheres resides at 500 nm.[39] This result confirms the general trend predicted by our DDA calculations that nanostructures with sharp corners display red-shifted extinction peaks, and that the number of peaks exhibited by a nanostructure increases with the number of ways it can be polarized.

Br^- is less corrosive than Cl^-, so if NaBr is added in place of NaCl there is still enough etching to eliminate the multiply twinned particles, but particles with only a single twin survive intact.[40] Figure 5A is a high-resolution TEM image of a single twinned seed, in which the {111} lattice fringes reflect across the twin plane. A zoomed-out view of the same particle is given in the inset to illustrate its spherical profile, with a twin plane

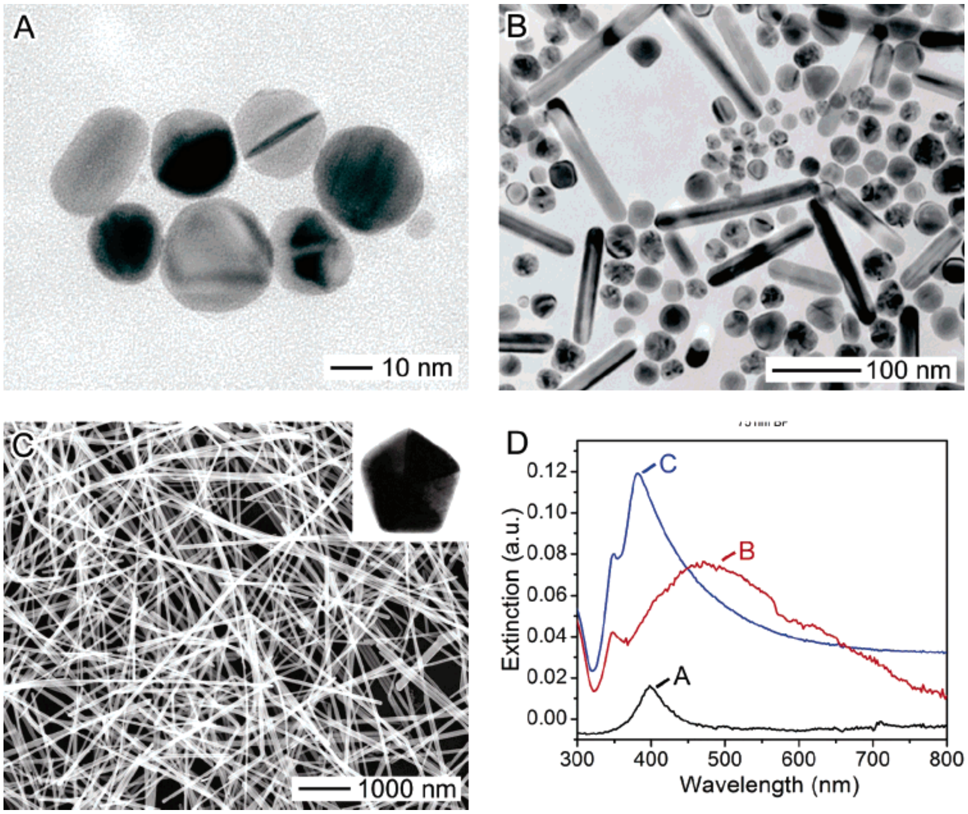

Figure 6. (A) TEM image of multiply twinned seeds present at 10 min in a nanowire reaction, to which Fe(acac)$_2$ and NaCl were added. Twins may not be clearly delineated depending on the particle orientation, but the shape and difference in contrast across the seeds indicates the presence of twin planes. (B) By 30 min, TEM shows the presence of nanorods along with twinned particles. (C) SEM image of nanowires at 60 min. The inset is a TEM image taken from a microtomed cross-section of a nanowire, displaying its internal 5-fold twinned crystal structure and pentagonal profile. (D) UV−vis extinction spectra of the samples taken during the reaction, illustrating how the SPR features evolved as the twinned nanoparticles grew into nanorods and nanowires. For additional results, see refs 32 and 41.

in the middle. These single twinned seeds grew to form right bipyramids 75 nm (Figure 5B) or 150 nm (Figure 5C) in edge length in a reaction stopped at 3 or 5 h, respectively, with edge length measured along one of the three edges that meet in a 90° angle. Figure 5D compares the normalized extinction spectra of these two different bipyramid sizes. The most intense dipole resonance peak of the 75-nm bipyramids is 100 nm red-shifted from that of the truncated nanocubes, again vindicating DDA calculations that predict corner sharpening causes resonance peaks to red-shift. The most intense peak shifts from 530 to 742 nm as the bipyramid grows to 150 nm because of increased charge separation and energy losses in the larger particle. These bipyramids are unique because they have corners significantly sharper than those of nanocubes where the two halves of the bipyramid meet, and thus could improve localized field enhancement for Raman scattering.

Silver nanowires can be grown from multiply twinned seeds in the presence of Cl$^-$ if etching is prevented.[41] Etching can be prevented either by running the reaction under argon, or by simply adding Fe(II) or Fe(III) at a molar ratio of Ag:Fe = 11 000. Figure 6A shows a TEM image of the multiply twinned particles produced at 10 min when both iron(II) acetylacetonate (Fe(acac)$_2$) and Cl$^-$ were added to the reaction. Multiply twinned decahedrons will not appear under TEM as illustrated in Figure 3 unless viewed along the {110} axis, but they can nonetheless be identified by the difference in contrast across the particle.[42] By 30 min, TEM showed that many of the multiply twinned decahedrons had grown into nanorods approximately 20 nm in diameter and 150 nm in length (Figure 6B). These nanorods rapidly grew longitudinally into micrometer-long nanowires by 60 min (Figure 6C). A TEM image of a microtomed cross-section of a nanowire in the inset shows its 5-fold twinned crystal structure and pentagonal profile.[32]

The transformation from twinned decahedrons into pentagonal nanowires could also be followed by taking UV−vis extinction spectra of reaction samples. Figure 6D shows that at 10 min the multiply twinned particles had an extinction spectrum similar to that of nanospheres, with a resonance peak at 400 nm. As multiply twinned decahedrons grew to form nanorods, their extinction peak shifted to 470 nm due to increased charge separation along the long axis of the nanorod. The mixture of nanostructures with different sizes and shapes contributes to the broadness of the peak in this spectrum. As the nanorods grow to become nanowires, the extinction band continues to broaden, but the most intense resonance peak blue-shifts back to ∼382 nm, similar to the spectra of silver films.[43]

It should now be clear that well-defined nanostructures of silver are obtained by controlling the crystal structure of the seeds from which they grow. Etching by oxygen and Cl$^-$ allows only single-crystal seeds to form, which can be grown quickly into sharp nanocubes, or slowly into truncated nanocubes. Moderate etching in the presence of Br$^-$ produces seeds with a single twin, which further grow to form right bipyramids. The absence of etching enables formation of the thermodynamically favored, multiply twinned, decahedron seeds, and their growth into pentagonal nanowires. Each of these nanostructures results from preferential formation of (100) facets on the seeds, which can be selectively stabilized thanks to a stronger interaction with PVP. Tetrahedra, octahedra, and large decahedra could also be produced by introducing a capping agent capable of stabilizing the (111) facets. Already seeds with parallel stacking faults have been grown into triangular and circular nanoplates through enlargement of (111) facets.[44] Exotic new shapes that are as yet unpredicted may also result through careful regulation of reduction kinetics and the controlled addition of atoms to specific facets.

Sensing with Silver Nanostructures

New ways to detect and quantify biological molecules with at least picomolar sensitivity are required for lab-on-a-chip detection of biomarkers for diseases, monitoring of chemical and biological agents, and for the construction of a complete model of cell functions. This is where silver nanostructures will likely play their most important role. In 2003, Van Duyne and co-workers demonstrated that the detection limit of a LSPR sensor based on a single nanoparticle was below 1000 small molecules (<2 zeptomoles), and approached the single-molecule limit for larger biomolecules.[45] They then made a LSPR biosensor that is the first sensitive enough to provide a clinical diagnosis of Alzheimer's disease through detection of amyloid-β derived diffusible ligand (ADDL) biomarkers in cerebrospinal fluid.[46] An LSPR sensor is based on the principle that the wavelength of light scattered by silver nanostructures depends on their local dielectric environment.[47] When an analyte adsorbs onto a nanostructure, its resonance peaks shift to a degree that correlates to the concentration of analyte.

Control of nanostructure shape allows the LSPR sensor to be optimized for even greater sensitivity. In a recent study it was found that 30-nm silver cubes have a single dipole resonance in water, but the resonance splits into two peaks in the spectrum of a single nanocube on a glass substrate.[48] Figure 7A displays the results of a finite-difference time-domain (FDTD) calculation that illustrates this phenomenon. As the nanocube approaches the substrate, its dipole resonance broadens and splits into a peak at 430 nm associated with large fields away from the substrate, and a peak at 550 nm associated with large fields toward the substrate. The calculation is performed for a 90-nm cube because peak splitting for the 30 nm nanocube is observed only when it is nearly touching the substrate. A figure of merit (FOM = m [eV RIU^{-1}]/ fwhm [ev]) was defined to compare the nanocube with other LSPR sensing platforms, where m is the measured shift of the resonance peak per refractive index unit (RIU), and fwhm is the full width at half-maximum of the resonance peak. The FOM is 5.4 for the sharp nanocube peak at 430 nm, a significant improvement on the FOM of ~3 for triangular nanoprisms. Thus the nanocube could lower the already incredible detection limit of LSPR sensors, extending their utility in biomedical research.

A second molecular sensing method that is inextricably linked to nanostructured silver is surface-enhanced Raman spectroscopy (SERS).[5] Every molecule has a distinct Raman spectrum that results from its characteristic vibrational energies, but this spectrum is usually too weak to detect. Fortunately, the intense local electric fields exhibited by silver nanostructures can enhance the Raman spectrum of adsorbed molecules by several thousand times. The degree of Raman enhancement is strongly dependent on the shape of the nanostructure substrate. To study this relationship, we heated 60-nm silver cubes (Figure 8A) in a 1 mM HCl in EG solution at 145 °C for 5 min to round their corners and edges (Figure 8B).[49] Corner and edge truncation caused the resonance peak of the nanocubes to blue-shift (Figure 8C), as is predicted by our calculations. The effect of truncation on Raman enhancement was observed by performing SERS on separate solutions of sharp and rounded nanocubes, each of which contained 0.929 m^2/L Ag and 2.86 μM 1,4-benzenedithiol (just enough for a complete monolayer), with laser excitation at 785 nm. The sharp cubes enhanced the intensity of the Raman spectrum of 1,4-benzenedithiol by 49 000 times, but this decreased by nearly half, to 27 000 times, after rounding.[50] One reason for this decrease in enhancement can be found in the UV−vis extinction spectra of these nanostructures, as the sharp cubes scatter and absorb light due to plasmon resonance at 785 nm, the wavelength of the laser, but the rounded cubes do not. In addition, sharp corners should provide greater localized electric field enhancement than rounded ones.[51] Thus it is critical to control the morphology of silver nanostructures if the Raman enhancement is to be optimized for sensing applications. Genetic diagnostics, immunoassay labeling, and detection of trace amounts of anthrax, glucose, and pesticides are just a few of the applications that have benefited from SERS.[6] Future SERS sensing platforms may include well-defined assemblies of sharp nanostructures to further improve the sensitivity and reliability of this exciting analytic tool.[51]

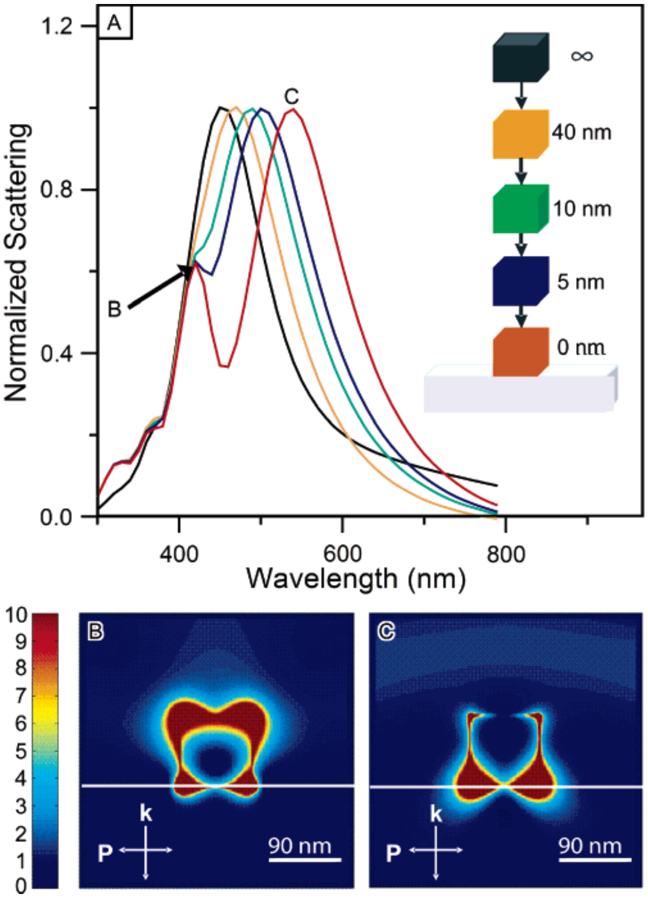

Figure 7. (A) The results of a finite-difference time-domain (FDTD) simulation illustrating how the extinction peak of a 90-nm cube splits as the nanocube approaches a glass substrate. (B) The peak at 430 nm is associated with near-fields away from the substrate. (C) The peak at 550 nm is associated with near-fields impinging on the substrate. A white line represents the substrate in (B) and (C). See ref 48 for detailed discussion.

Summary

Surface plasmon resonance is tedious to describe mathematically, Gustav Mie's paper on particle scattering contains no less than 102 sets of equations, but it can be understood conceptually as the oscillation of free electrons in phase with incident light, with induced surface charges providing the main restoring force

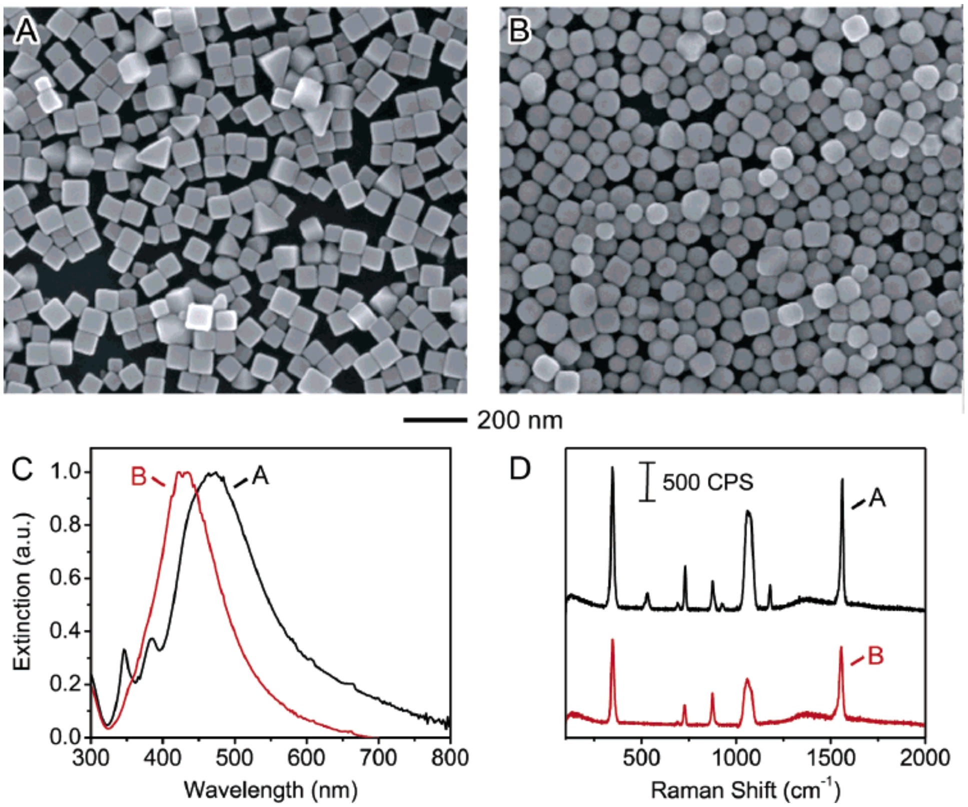

Figure 8. SEM of (A) sharp and (B) rounded nanocubes. (C) UV−vis extinction spectra of sharp and rounded nanocubes, illustrating how the resonance blue-shifts after corner truncation. (D) SERS spectra obtained from solutions of sharp and rounded nanocubes, each of which contained 0.929 m^2/L Ag and 2.86 μM 1,4-benzenedithiol (just enough for a complete monolayer), with laser excitation at 785 nm. The sharp cubes enhanced the intensity of the Raman spectrum of 1,4-benzenedithiol by 49 000 times, but this decreased by nearly half, to 27 000 times, after rounding. Additional work is reported in ref 49.

for oscillation. In a series of DDA calculations, we have explored how changes in the morphology of a silver nanostructure modify the wavelengths and intensity of light scattered or absorbed. All morphologically induced spectral shifts were explained in terms of the effect of shape on surface polarization because, much like a weight on a spring determines its period and amplitude of oscillation, polarization determines the frequency and dipole moment of electron oscillations, and thus the frequency and intensity of light scattered or absorbed. The goal of this approach was to build on readers' knowledge of Coulombic forces to facilitate an intuitive understanding of the relationship between the shape of a nanostructure and its optical properties.

Production of well-defined silver nanostructures is no trivial matter, but it can be achieved by controlling the seeds from which nanostructures grow. Here we have showed how three types of seeds with distinct crystal structures can be selected through etching, and then grown to produce the morphology of choice. The effect of anisotropy and corner sharpness on plasmon resonance was clearly apparent after examination of the UV−vis extinction spectra of synthesized nanostructures, validating the calculated predictions. It was further demonstrated how controlling the shape of a nanostructure can improve the sensitivity of both LSPR and SERS sensing platforms through finer control of the frequency of the light scattered by a nanostructure and greater enhancement of local electric fields.

This is an exciting time to be working with plasmonic nanostructures, because the field is truly in its infancy. The majority of well-defined silver nanostructures have been produced in the past five years, and the work of characterizing their optical properties has only just begun. Indeed, it remains a challenge to correlate the precise shape and size of a synthesized nanostructure with its optical properties, as shape is accurately characterized by electron microscopy, while optical characterization requires finding the same nanostructure in the optical microscope. In-depth characterization would be easier to perform if nanostructures assembled onto a substrate in a predictable manner. Achieving this will likely require functionalization of nanostructures with molecules that attract them to specific locations on a patterned surface. Finding ways to predictably assemble plasmonic nanostructures onto a surface will not only facilitate their characterization but also enable high-throughput, solution-phase production of nanostructure arrays for sensing, spectroscopy, and the guiding of light at the nanoscale.

Acknowledgment. This work has been supported in part by the NSF (DMR-0451788), a subcontract from the NSF-funded MERSEC program at the UW, a fellowship from the David and Lucile Packard Foundation, and a TGIF grant from the UW TechTransfer Office. Y.X. is a Camille Dreyfus Teacher Scholar and an Alfred P. Sloan Research Fellow. B.W. thanks the Center for Nanotechnology at the UW for an IGERT Fellowship funded by NSF and NCI. S.H.I. was partially supported by a postdoctoral fellowship from the KOSEF. Z.Y.L. is supported by the National Natural Science Foundation of China (No. 10525419). Electron microscopic studies were performed at the UW Nanotech User Facility, a member of the National Nanotechnology Infrastructure Network (NNIN) supported by the NSF.

References and Notes

(1) Faraday, M. *Philos. Trans. R. Soc. London* **1857**, *147*, 145.

(2) Kreibig, U.; Vollmer, M. *Optical Properties of Metal Clusters*, Springer: New York, 1995; Chapter 2.

(3) Cooper, M. *Nat. Rev. Drug Discov.* **2002**, *1*, 515.

(4) McFarland, A. D.; Van Duyne, R. P. *Nano Lett.* **2003**, *3*, 1057.

(5) Jeanmaire, D. L.; Van Duyne, R. P. *J. Electroanal. Chem.* **1977**, *84*, 1.

(6) Haynes, C. L.; McFarland, A. D.; Van Duyne, R. P. *Anal. Chem.* **2005**, 338A.

(7) Maier, S. A.; Kik, P. G.; Atwater, H. A.; Meltzer, S.; Harel, E.; Koel, B. E.; and A. A. G. Requicha *Nature Mater*. **2003**, *2*, 229.

(8) Lezec, H. J.; Degiron, A.; Devaux, E.; Linke, R. A.; Martín-Moreno, L.; García-Vidal, F. J.; Ebbesen, T. W. *Science* **2002**, *297*, 820.

(9) Barnes, W. L.; Dereux, A.; Ebbesen, T. W. *Nature* **2003**, *424*, 824.

(10) Hubert, C.; Rumyantseva, A.; Lerondel, G.; Grand, J.; Kostcheev, S.; Billot, L.; Vial, A.; Bachelot, R.; Royer, P.; Chang, S.-h.; Gray, S. K.; Wiederrecht, G. P.; Schatz, G. C. *Nano Lett.* **2005**, *5*, 615.

(11) Fang, N.; Lee, H.; Sun, C.; Zhang, X. *Science* **2005**, *308*, 534.

(12) Yguerabide, J.; Yguerabide, E. E. *Anal. Biochem.* **1998**, *262*, 137.

(13) Quniten, M. *Appl. Phys. B* **2001**, *73*, 245.

(14) Mie, G. *Anal. Phys.* **1908**, *25*, 376.

(15) Draine, B. T.; Flatau, P. J. *J. Opt. Soc. Am. A* **1994**, *11*, 1491.

(16) Fuchs, R. *Phys. Rev. B* **1975**, *11*, 1732.

(17) Haes, A. J.; Haynes, C. L.; McFarland, A. D.; Schatz, G. C.; Van Duyne, R. P.; Zou, S. *MRS Bull.* **2005**, *30*, 368.

(18) Kottmann, J. P.; Martin, O. J. F.; Smith, D. R.; Schultz, S. *Phys. Rev. B* **2002**, *64*, 235402.

(19) Aizpurua, J.; Bryant, G. W.; Richter, L. J.; García de Abajo, F. J.; Kelley, B. K.; Mallouk, T. *Phys. Rev. B* **2005**, *71*, 235420.

(20) Kelly, K. L.; Coronado, E.; Zhao, L. L.; Schatz, G. C. *J. Phys. Chem. B* **2003**, *107*, 668.

(21) Prodan, E.; Radloff, C.; Halas, N. J.; Norlander, P. *Science* **2003**, *302*, 419.

(22) Schelm, S.; Smith, G. B. *J. Phys. Chem. B* **2005**, *109*, 1689.

(23) Teperik, T. V.; Popov, V. V.; García de Abajo, F. J. *Phys. Rev. B.* **2004**, *69*, 155402.

(24) Aizpurua, J.; Hanarp, P.; Sutherland, D. S.; Käll, M.; Bryant, G. W.; García de Abajo, F. J. *Phys. Rev. Lett.* **2003**, *90*, 057401.

(25) Jin, R.; Cao, Y.; Mirkin, C. A.; Kelly, K. L.; Schatz, G. C.; Zheng, J. G. *Science* **2001**, *294*, 1901.

(26) Chen, S.; Fan, Z.; Carroll, D. L. *J. Phys. Chem. B* **2002**, *106*, 10777.

(27) Jana, N. R.; Gearheart, L.; Murphy, C. J. *Chem. Commun.* **2001**, 617.

(28) Fiévet, F.; Lagier, J. P.; Figlarz, M. *MRS Bull.* **1989**, *14*, 29.

(29) (a) Sun, Y.; Xia, Y. *Science* **2002**, *298*, 2176. (b) Sun, Y.; Xia, Y. *Adv. Mater.* **2002**, *14*, 833. (c) Sun, Y.; Yin, Y.; Mayers, B.; Herricks, T.; Xia, Y. *Chem. Mater.* **2002**, *14*, 4736. These and all previous studies may have been affected by ionic contaminants in the EG, as they were performed before this issue was recognized.

(30) (a) Wiley: B.; Sun, Y.; Mayers, B.; Xia, Y. *Chem. Eur. J.* **2005**, *11*, 454. (b) Wiley: B.; Sun, Y.; Chen, J.; Cang, H.; Li, Z.-Y.; Li, X.; Xia, Y. *MRS Bull.* **2005**, *30*, 356.

(31) (a) Sun, Y.; Gates, B.; Mayers, B.; Xia, Y. *Nano Lett.* **2002**, *2*, 165. (b) Washio, I.; Xiong, Y.; Yin, Y.; Xia, Y. *Adv. Mater.* **2006**, *45*, 1288.

(32) Sun, Y.; Mayers, B.; Herricks, T.; Xia, Y. *Nano Lett.* **2003**, *3*, 955.

(33) Smith, D. J.; Petford-Long, A. K.; Wallenberg, L. R.; Bovin, J. O. *Science* **1986**, *233*, 872.

(34) Ajayan, P. M.; Marks, L. D. *Phys. Rev. Lett.* **1998**, *60*, 585.

(35) Wiley, B.; Herricks, T.; Sun, Y.; Xia, Y. *Nano Lett.* **2004**, *4*, 1733.

(36) Buatier de Moneot, F.; Cupolillo, A.; Valbusa, U.; Rocca, M. *Chem. Phys. Lett.* **1997**, *270*, 345.

(37) (a) Xiong, Y.; Chen, J.; Wiley, B.; Xia, Y.; Aloni, S.; Yin, Y. *J. Am. Chem. Soc.* **2005**, *127*, 7332. (b) Xiong, Y.; Wiley, B.; Chen, J.; Xia, Y.; Yin, Y.; Li, Z.-Y. *Nano Lett.* **2005**, *5*, 1237. (c) Chen, J.; Herricks, T.; Xia, Y. *Angew. Chem., Int. Ed.* **2005**, *44*, 2589. (d) Zettsu, N.; McLellan, J. M.; Wiley, B.; Yin, Y.; Li, Z.-Y.; Xia, Y. *Angew. Chem., Int. Ed.* **2006**, *45*, 1288.

(38) Im, S. H.; Lee, Y. T.; Wiley, B.; Xia, Y. *Angew. Chem., Int. Ed.* **2005**, *44*, 2154.

(39) Evanoff, D. D., Jr.; Chumanov, G. *Chem. Phys. Chem.* **2005**, *6*, 1221.

(40) Wiley, B. J.; Xiong, Y.; Li, Z.-Y.; Yin, Y.; Xia, Y. *Nano Lett.* **2006**, *6*, 765.

(41) Wiley, B.; Sun, Y.; Xia, Y. *Langmuir* **2005**, *21*, 8077.

(42) Wang, Z. L. *J. Phys. Chem. B* **2000**, *104*, 1153.

(43) Neff, H.; Henkel, S.; Sass, J. K.; Steinbeiss, E.; Ratz, P.; Müller, J.; Michalke, W. *J. Appl. Phys.* **1996**, *80*, 1058.

(44) Lofton, C.; Sigmund, W. *Adv. Funct. Mater.* **2005**, *15*, 1197.

(45) McFarland, A.; VanDuyne, R. P. *Nano Lett.* **2003**, *3*, 1057.

(46) Haes, A. J.; Chang, L.; Kleing, W. L.; Van Duyne, R. P. *J. Am. Chem. Soc.* **2005**, *127*, 2264.

(47) Haes, A. J.; Van Duyne, R. P. *Anal. Bioanal. Chem.* **2004**, *379*, 920.

(48) Sherry, L. J.; Chang, S. H.; Schatz, G. C.; Van Duyne, R. P.; Wiley, B. J.; Xia, Y. *Nano Lett.* **2005**, *5*, 2034.

(49) McLellan, J.; Siekkinen, A.; Chen, J.; Xia, Y. *Chem. Phys. Lett.* **2006**, in press.

(50) Enhancement is based on the integrated intensity of the 8a band at 1565 cm^{-1} as compared to the Raman spectrum of a 0.1 M solution of 1,4-benzenedithiol in 12 M NaOH.

(51) Zou, S.; Schatz, G. C. *Chem. Phys. Lett.* **2005**, *403*, 62.